energies

MDPI

Article

Catalysts for ORR Based on Silver-Modified Graphene Oxide and Carbon Nanotubes

Kirill Yurievich Vinogradov [1], Roman Vladimirovich Shafigulin [1], Elena Olegovna Tokranova [1], Sergey Vladimirovich Vostrikov [2], Evgeniya Andreevna Martynenko [2], Vladimir Vladimirovich Podlipnov [1], Pavel Vladimirovich Kazakevich [3], Artem Anatolevich Sheldaisov-Meshcheryakov [2], Nikolai Aleksandrovich Vinogradov [2] and Andzhela Vladimirovna Bulanova [1,*]

[1] Institute of Natural Sciences, Samara University, 443086 Samara, Russia
[2] Chemical Engineering Faculty, Samara State Technical University, 443100 Samara, Russia
[3] Samara Branch of P.N. Lebedev Physical Institute, Russian Academy of Sciences, 443011 Samara, Russia
* Correspondence: av.bul@yandex.ru

Abstract: The main obstacle to the widespread dissemination of fuel cells is the high cost, so researchers are actively searching for ways to replace the expensive platinum catalyst with cheaper analogs. In this paper we studied the Ag- and Pd-containing carbon catalysts based on carbon nanotubes and graphene oxide. The study of the textural characteristics of the catalysts showed that the greatest specific surface area has a catalyst based on MWCNT containing 10% silver, all synthesized catalysts are mainly mesoporous, and the content of micropores is insignificant. Raman spectroscopy and SEM data indicate a significant change in the structure of the modified carriers compared to pure MWCNT and GO. An electrochemical experiment was performed and linear voltammetric diagrams were obtained and compared with the voltammetric diagrams obtained on the platinum catalyst. GO_Ag 10% and MWCNT_Ag 10% Pd 10% are closest in the values of kinetic parameters in both kinetic and diffusion regions. GO_Ag 10% has the highest initial potential E_{onset} = −0.145 V and MWCNT_Ag 10% Pd 10% has the highest half-wave potential E1/2 = −0.23 V. The studied catalysts have characteristics comparable to those presented in the literature.

Keywords: electrochemical oxygen reduction; palladium; silver; ORR; carbon nanotubes; graphene oxide; bimetallic electrocatalysts

Citation: Vinogradov, K.Y.; Shafigulin, R.V.; Tokranova, E.O.; Vostrikov, S.V.; Martynenko, E.A.; Podlipnov, V.V.; Kazakevich, P.V.; Sheldaisov-Meshcheryakov, A.A.; Vinogradov, N.A.; Bulanova, A.V. Catalysts for ORR Based on Silver-Modified Graphene Oxide and Carbon Nanotubes. *Energies* **2023**, *16*, 1526. https://doi.org/10.3390/en16031526

Academic Editor: Jun Li

Received: 13 January 2023
Revised: 25 January 2023
Accepted: 1 February 2023
Published: 3 February 2023

1. Introduction

Currently, more and more attention is being paid to alternative, more environmentally friendly sources of energy. Fuel cells (FC) can serve as such sources. Currently, fuel cells are widespread in the automotive, shipbuilding, and aircraft industries. Fuel cells are used as stationary energy sources. The most promising application of fuel cells is in mobile and portable devices.

Fuel cells are based on the oxygen reduction reaction. Due to the high degree of irreversibility, the speed of this reaction is very low, so for further promising applications it is necessary to use efficient catalysts. The high cost of platinum catalysts used increases the cost of fuel cells and complicates their widespread use [1]. Therefore, the creation of effective and less expensive catalysts with a minimal content of precious metals is one of the most promising directions in the development of inexpensive fuel cells.

In recent years, the search for non-platinum catalysts or catalysts with a reduced content of platinum on a carbon base is conducted more and more actively [2–6]. Along with the search for inexpensive effective ORR catalysts, research is conducted on the selection of optimal carriers for them [7,8]. Carbon black is the most commonly used carrier, but studies show that the use of carbon nanotubes (CNTs), graphene oxide (GO), and their doped forms can produce catalysts with characteristics superior to those previously created [9,10].

Palladium, silver, and other transition metals and their alloys, as well as bimetallic catalysts containing a minimal amount of platinum are used as modifiers [11–13]. Thus, bimetallic catalysts based on silver and platinum obtained sonochemically on CNTs were studied, and the authors showed that the ORR proceeded along the four-electron path [14]. CNT-based catalysts showed better results than carbon black-based catalysts. However, both types of systems had a sufficiently high activity.

The properties of electrocatalytic systems containing silver on several carbon carriers at once were studied [15]. To do this, authors conducted electrodeposition of Ag on four electrodes made of carbon black, graphene, CNTs, and graphene oxide doped with nitrogen, and then used them in the oxygen reduction reaction. The best properties were shown by the catalyst based on GO doped with nitrogen. The reduction reaction of oxygen using systems containing silver proceeded according to the four-electron mechanism. However, the activity of these catalysts is less than that of platinum-based catalysts.

The aim of this work was to study the activity of electrochemical oxygen reduction (ORR) catalysts based on MWCNTs and GO modified with different amounts of silver and palladium. Four samples were prepared: GO_Ag 10%, GO_Ag 20%, MWCNT_Ag 10%, MWCNT_Ag 20%, and a fifth sample that contained the additional component palladium: MWCNT_Ag 10% Pd 10%. The purpose was to evaluate the effect on the ORR values of the mass silver content as well as the addition of a small amount of palladium.

2. Materials and Methods

2.1. Chemicals and Materials

The following materials were used in the course of the study: Multiwalled carbon nanotubes (>95% carbon, diameter 50–90 nm, Aldrich, St. Louis, MO, USA), graphene oxide (Rusgraphene, Moscow, Russia), silver nitrate (Aldrich), potassium chloride (Aldrich), and palladium chloride (abcr). A commercial platinum catalyst from HiSPEC with a platinum content of 20 wt% was used as a reference sample.

2.2. Synthesis of Catalysts

Accurate weights of carbon carriers (0.2 g MWCNT or GO) and the calculated amount of silver nitrate were dissolved in 50 mL of ethanol by ultrasonic dispersion for 4 h. The resulting suspension was dried at 90 °C in a muffle furnace, and then the dry residue was pyrolyzed in an inert (nitrogen) atmosphere at 600 °C for an hour. Heating was performed at a rate of 5 °C/min, followed by a step of 600 °C for 1 h. As a result, catalysts GO_Ag 10%, GO_Ag 20%, MWCNT_Ag 10%, and MWCNT_Ag 20% were obtained. To prepare the MWCNT_Ag 10% Pd 10% catalyst, MWCNT_Ag 10% and palladium chloride were dissolved, followed by pyrolysis at 900 °C according to the same scheme.

2.3. Preparation of Catalytic Ink

A sample of the catalyst (0.2 g) and 200 μL of Nafion were dissolved in 10 mL of ethanol using ultrasonic dispersion-homogenization for 2 h. The resulting ink was applied to a disk electrode (S = 0.071 cm^2) with a load of 80 μg/cm^2 and then dried at 90 °C for 8 h.

2.4. Characteristics of Catalysts

Using a highly sensitive gas sorption analyzer micropore-porosimeter Quantochrome Autosorb-1 (Quantachrome Instruments, Boynton Beach, FL, USA) for supports and catalysts obtained, information was obtained on the textural characteristics of materials: specific surface area, pore volume, and pore diameter. The specific surface area of the samples was determined by the Brunauer–Emmett–Teller (BET) model.

Raman spectral analysis was carried out in backscattering mode using a Renishaw InVia micro-Raman spectrometer equipped with a charge-coupled detector (CCD), a 532 nm 1–5 mW Ar-ion laser focusing on a spot with a diameter of 2 μm, a diffraction grating with a density of 1800 lines/mm, and a spectral resolution of 1 cm^{-1}.

The study of the morphology of carrier particles and the resulting catalysts was carried out on a CarlZeiss Supra 25 scanning electron microscope using the SEM method.

2.5. Electrochemical Experiment

The electrochemical oxygen reduction reaction in an alkaline medium was studied in a 0.1 M potassium hydroxide solution by the potentiometric method on a CorrTest CS120 potentiostat-galvanostat. The work was carried out in a glass three-electrode cell for VED-06 with a rotating disk electrode with an OrigaTrod Lt potentiometer. The auxiliary electrode was a platinum electrode with a large specific surface area. The reference electrode was a silver chloride electrode. The removal of linear voltammograms was carried out in a 0.1 M KOH solution saturated with oxygen in the voltage range of $-0.8 \div 0.2$ V with a sweep of 5 mV/s and a disk electrode rotation speed of 500–2500 rpm. Oxygen saturation was performed for 1 h using an oxygen concentrator. Linear voltammetry was taken after stabilizing the electrochemical system by cycling 50 times in the operating voltage range. Linear voltammetry images were taken at least 5 times until the results converged. The error in determining the parameters was not more than two percent. Cyclic voltammograms were obtained in a solution deaerated by nitrogen bubbling in the voltage range of $-1 \div 0.2$ V. During the cyclic voltammetry process, a nitrogen current was passed over the reaction solution.

3. Results and Discussion

As a result of studying the samples by the method of low-temperature adsorption–desorption of nitrogen, the textural characteristics of the supports and the synthesized catalysts were obtained. The adsorption–desorption isotherms of the studied samples are shown in Figure 1, and the textural characteristics are presented in Table 1.

The obtained isotherms can be attributed to type II adsorption isotherms according to the IUPAC classification, which indicates the presence of macropores and mesopores in the material [16]. You can also see a hysteresis loop at high pressures, which can be caused by capillary condensation, which makes it possible to classify the studied materials as mesoporous.

According to the results of BET analysis, the total specific surface area of the synthesized MWCNT-based catalysts is about 20 m^2/g, which exceeds the specific surface area of the original MWCNTs (~15 m^2/g), and may be due to partial decomposition of the support during synthesis [17].

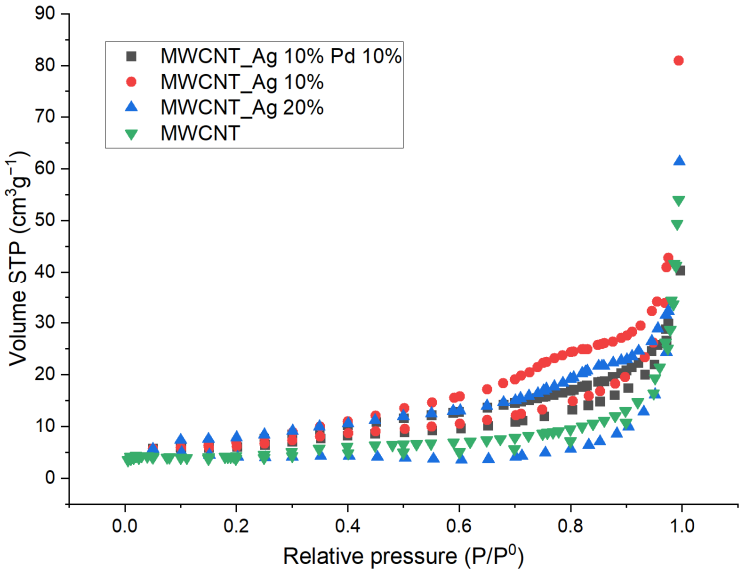

Figure 1. Isotherms of low-temperature adsorption–desorption of nitrogen on the investigated catalysts and carriers.

Table 1. The textural characteristics of the supports and catalysts.

Sample	Surface Area, S_{BET}, m^2/g	Pore Volume, V_P, cm^3/g	Pore Diameter, Dv(d),nm
MWCNT	14.9	0.08	3.4
GO_Ag 10% [1]	-	-	-
GO_Ag 20% [1]	-	-	-
MWCNT_Ag 10%	21.8	0.12	3.8
MWCNT_Ag 20%	11.5	0.09	8.6
MWCNT_Ag 10% Pd 10%	20.8	0.05	3.4

[1] It was not possible to take isotherms for technical reasons.

It is shown that the sample of bimetallic catalyst based on carbon nanotubes MWCNT_Ag 10% Pd 10% is characterized by the smallest volume and pore diameter. The mass loading of silver monometallic catalyst based on nanotubes decreases the specific surface area of the material relative to the unmodified sample.

Additional information about the structure of the studied catalysts can be obtained from the Raman spectrum of the samples presented in Figure 2.

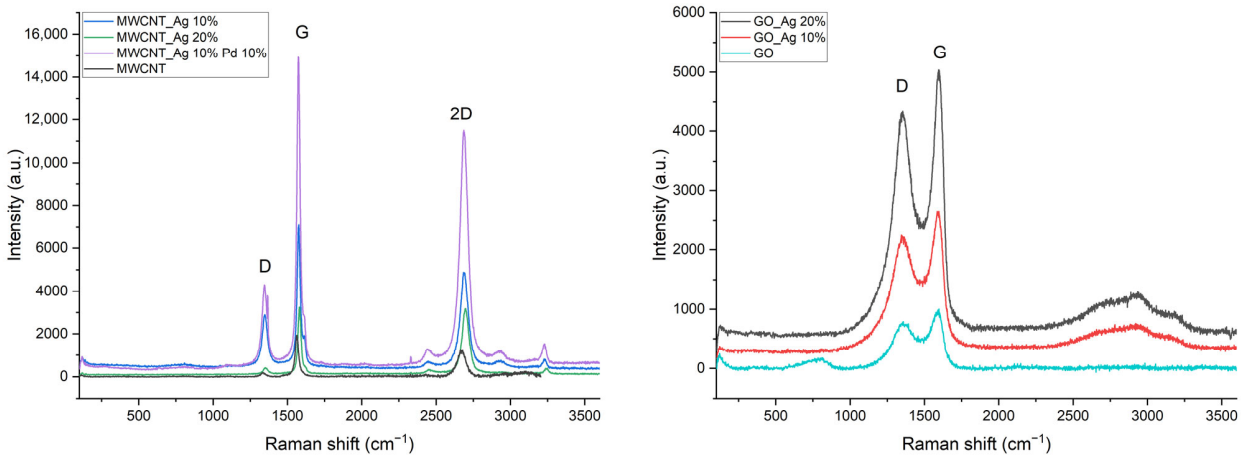

(**a**) (**b**)

Figure 2. Raman spectra of synthesized samples and initial carbon supports: (**a**) MWCNT materials, (**b**) GO materials.

The spectrum clearly shows peaks characteristic of carbon materials: the peak of disordered carbon (1330 cm^{-1}—D-band) and the peak of graphite carbon (1590 cm^{-1}—G-band). The process of doping carbon materials often leads to the formation of defects and, as a result, to a decrease in the ordering of the material. The results of the Raman spectral analysis performed are shown in Table 2.

As a result of the modification of carbon materials with metals, the characteristic bands shift and the IG/ID ratio decreases. There is also a shift in the characteristic 2D band and an increase in the I2D/IG ratio. Analyzing the Raman spectra for catalysts based on carbon nanotubes revealed that the samples MWCNT_Ag 10% and MWCNT_Ag 10% Pd 10% underwent the maximum change in structure. This indicates a denser interaction of metals with the carbon surface of the nanotubes. This can probably lead to an increase in the electronic conductivity of these samples and, consequently, enhance the catalytic properties in the oxygen reduction reaction. When graphene oxide was modified, no significant changes were observed in the spectrum, which is apparently due to the initially low degree of ordering of graphene oxide. However, some increase of defects in the sample during modification can be noted. In this case, the concentration of silver practically does not affect the depth of the defect formation process.

Table 2. Results of the Raman spectra of the synthesized catalysts and initial carbon supports.

Sample	ν(D), cm^{-1}	ν(G), cm^{-1}	ν(2D), cm^{-1}	ID	IG	I2D	IG/ID	I2D/IG
GO	1357	1598	-	791	1004	-	1.27	-
GO_Ag 10%	1345	1598	-	2241	2650	-	1.18	-
GO_Ag 20%	1355	1594	-	4341	5036	-	1.16	-
MWCNT	1336	1565	2666	187	1942	1273	10.39	0.66
MWCNT_Ag 10%	1350	1577	2684	2899	7108	4874	2.45	0.69
MWCNT_Ag 20%	1353	1580	2700	415	3248	3184	7.83	0.98
MWCNT_Ag 10% Pd 10%	1345	1573	2686	4310	14,933	11,393	3.46	0.76

In addition to the peaks belonging to different types of carbon, the appearance of a characteristic blurred peak in the region ~2940 cm^{-1} can be noticed on the samples of silver-modified catalysts. Unmodified samples of graphene oxide and carbon nanotubes lack this signal. These characteristic signals are especially prominent on the graphene oxide samples: the peak intensity increases with the increasing mass content of silver. This peak can serve as an indirect confirmation of the presence of silver nanoparticles in the synthesized materials—which are characterized by the presence of a group of peaks in the ~2800–3000 cm^{-1} region [18].

The morphology of the catalysts was studied by the SEM method, photographs of which are shown in Figure 3.

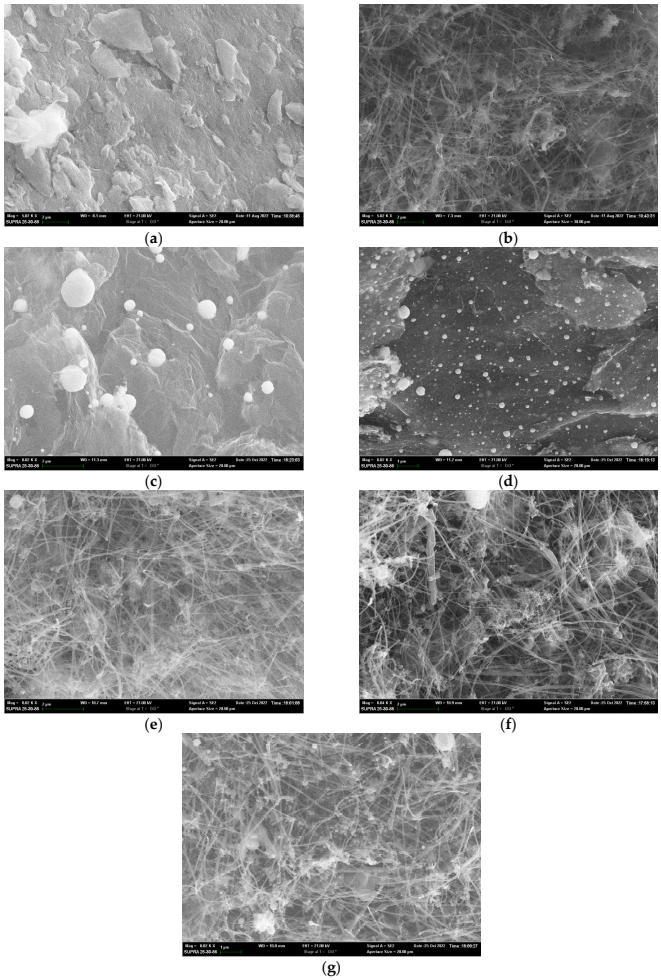

Figure 3. SEM photographs: (**a**) GO (magnification 5000 times); (**b**) MWCNT (magnification 5000 times); (**c**) GO_Ag 10% (magnification 8000 times); (**d**) GO_Ag 20% (magnification 8000 times); (**e**) MWCNT_Ag 10% (magnification 8000 times); (**f**) MWCNT_Ag 20% (magnification 8000 times); (**g**) MWCNT_Ag 10% Pd 10% (magnification 8000 times).

It can be observed from SEM photographs that GO is amorphous particles, while CNTs have the structure of thin intertwining tubes. During modification, the appearance of spherical metal particles uniformly distributed over the surface is observed on the catalyst surface. The sample catalyst based on graphene oxide with a mass loading of 10% (GO_Ag 10%) is characterized by a friable surface, compared with the GO_Ag 20% catalyst.

The size distribution of nanoparticles was carried out by post-processing of SEM images. The boundary of contrasting spherical formations was determined and the diameter of the particles within the boundaries of one frame was calculated. When analyzing images from CNTs, it is possible to identify only particles located on the surface of a carbon nanotube. For image post-processing and statistical data processing, ImageJ and Kompas 3D software products were used. The results of the analysis are shown in Figure 4.

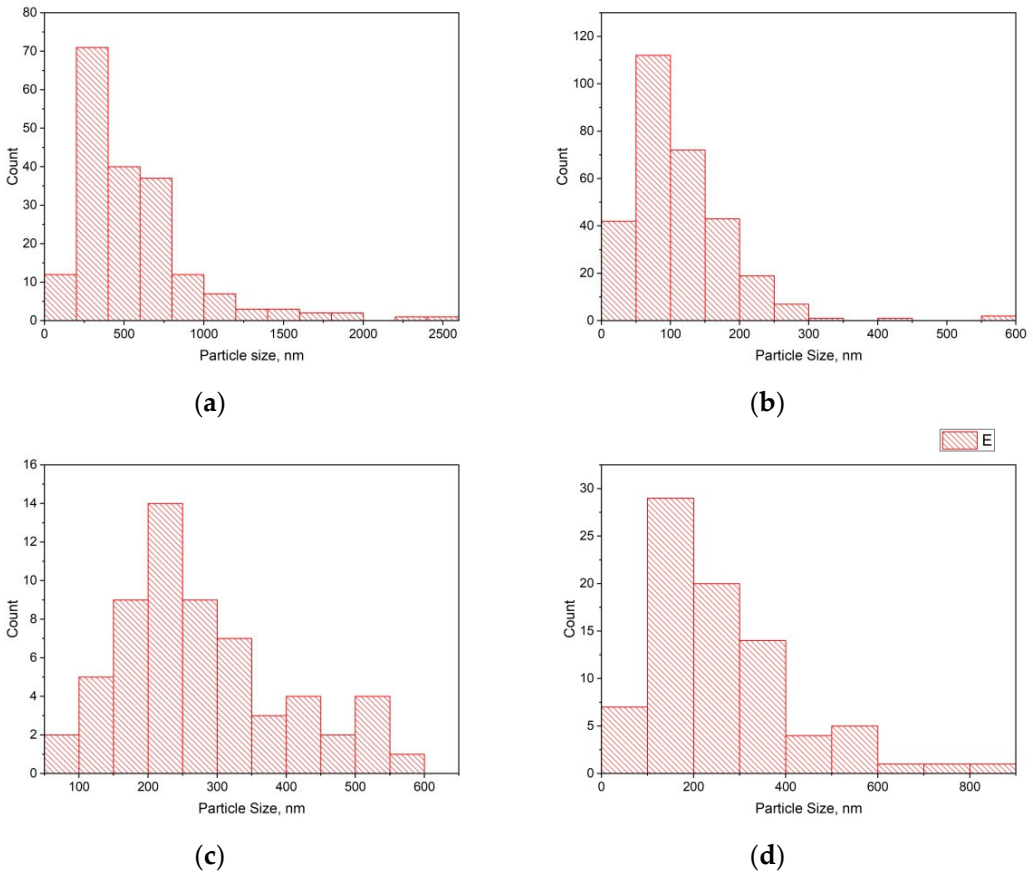

Figure 4. Distribution of metal particles by size on the catalyst: (**a**) GO_Ag 10%, (**b**) GO_Ag 20%, (**c**) MWCNT_Ag 10%, (**d**) MWCNT_Ag 10% Pd 10%.

The metal is on the surface in the form of spherical structures of various sizes: 50–100 nm for GO_Ag 20% and 200–400 nm for GO_Ag 10%. Larger metal particles are observed on GO_Ag 10%, despite the lower silver content. For MWCNT_Ag 10% and MWCNT_Ag 10% Pd 10% catalysts, the particle sizes are 200–250 nm and 150–200 nm, respectively.

X-ray fluorescence analysis was used for qualitative identification of metals. Figure 5 shows the spectra of the samples GO_Ag 10% and MWCNT_Ag 10% Pd 10%, on which the characteristic peaks of the corresponding metals are clearly visible.

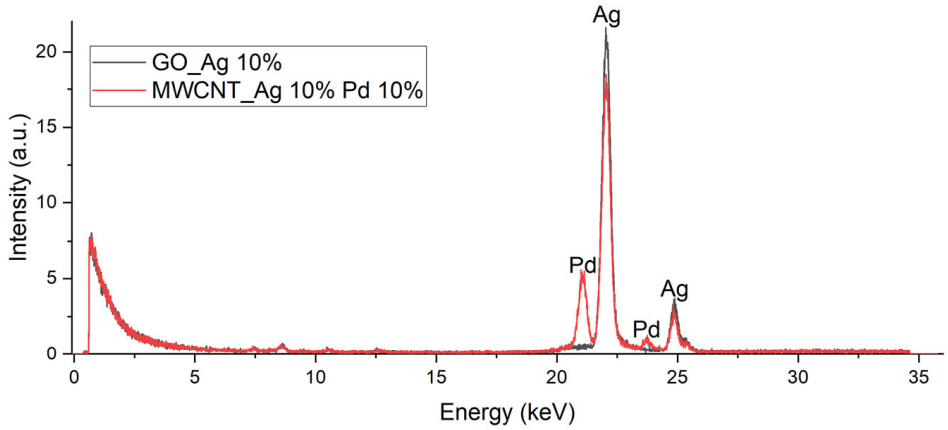

Figure 5. XRF spectrum of samples GO_Ag 10% and MWCNT_Ag 10% Pd 10%.

To study the effectiveness of the synthesized catalysts based on carbon nanotubes (CNTs) and graphene oxide (GO) an electrochemical experiment in the modes of linear and cyclic voltammetry was conducted. Figure 6 shows the results of linear voltammetry of the studied catalysts.

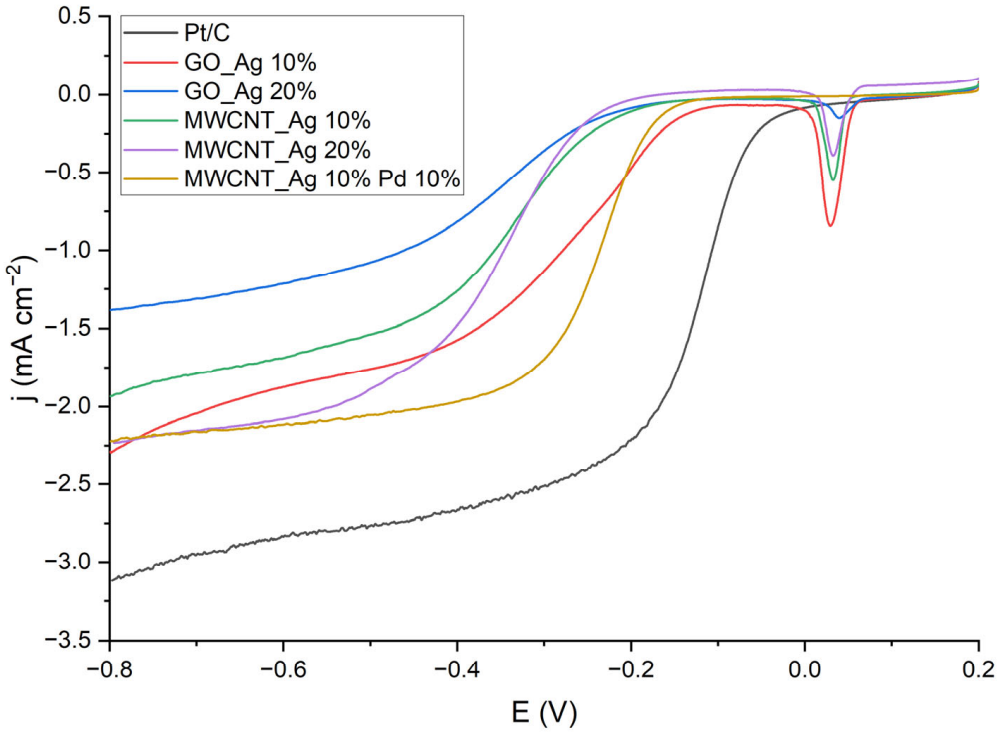

Figure 6. Linear voltammograms of the oxygen reduction reaction in a 0.1 M KOH solution saturated with oxygen on the test catalysts at an electrode rotation speed of 1000 rpm.

A number of factors were taken into account in the analysis of different carbon carriers:

1. The presence of surface oxygen-containing functional groups;
2. Specific surface area of the catalyst;
3. Porosity.

An increase in the number of surface oxygen-containing groups increases the adsorption of initial substances, which can reduce the activity of the catalyst. Increasing the specific surface area leads to improved catalytic properties. The accessibility of the active centers of the catalyst is related to porosity, so only powdered carbon materials were used. When comparing GO_Ag 20% and MWCNT_Ag 20%, it can be observed that GO-based

electrocatalysts have low activity in the oxygen reduction reaction compared to MWCNT. Apparently, this is due to the presence of a large number of surface oxygen-containing groups, which enhances the adsorption of initial compounds and poisons the surface. CNT-based samples exhibit high catalytic activity. This is probably due to the peculiarities of the MWCNTs structures and their high electronic conductivity. They exhibit almost metallic properties.

During the experiment the increased activity of GO_Ag 10% catalyst was revealed. The reasons for this phenomenon are being investigated.

The addition of 10% palladium in the MWCNT_Ag 10% Pd 10% catalyst significantly increases the activity of the catalyst, increases the initial potential and half-wave potential, and the limiting current becomes more pronounced.

As can be seen from the voltammograms made for the GO_Ag 10% catalyst shown in Figure 6, two waves are observed on the polarization curves, which can be caused by the electrical recovery of oxygen from an alkaline electrolyte with a step mechanism [19] where HO_2^- ions are initially formed at the first stage of the two-electron process, and then water molecules. Conversely, for other catalysts, only one pronounced plateau is observed on the polarization curves due to the four-electron mechanism of electrical recovery of oxygen from an alkaline electrolyte.

Kinetic and thermodynamic characteristics of the oxygen electroreduction reaction on synthesized catalysts are presented in Table 3.

Table 3. Parameters of the reaction of electroreduction of oxygen on synthesized catalysts.

Catalyst	E_{onset},V	E½,V	J_{kin}, mA/cm^2	J_{dif}, mA/cm^2
Pt/C	−0.035	−0.12	−0.2161	−3.12
GO_Ag 10%	−0.145	−0.27	−0.0700	−2.29
MWCNT_Ag 10%	−0.218	−0.33	−0.0264	−1.93
GO_Ag 20%	−0.237	−0.32	−0.0302	−1.38
MWCNT_Ag 20%	−0.246	−0.33	0.0294	−2.23
MWCNT_Ag 10% Pd 10%	−0.168	−0.23	−0.0149	−2.22

For better illustration, Figure 7 shows comparative diagrams of the obtained values for the synthesized catalysts.

All silver catalysts (except GO_Ag 10%) showed similar half-wave potential E½≈ −0.32 ÷ −0.33 V, but different initial potentials E_{onset} = −0.218 ÷ −0.246 V. The higher initial potential is observed for MWCNT_Ag 10%. Evaluating the catalytic properties of GO_Ag 10%, one can notice a significant increase in the half-wave potential E½ = −0.27 and the initial potential E_{onset} = −0.145, which may be due to the combined effect on the ORR surface of graphene oxide and silver nanoparticles. The MWCNT_Ag 20% catalyst showed the worst efficiency in the reaction of electroreduction of oxygen in alkaline electrolyte—it is characterized by the lowest values of the half-wave potential and the initial potential. This is probably due to the fact that this MWCNT_Ag 20% catalyst is characterized by the lowest specific surface area (11.5 m^2/g). At the same time, the pore volume and diameter of this catalyst are the largest (in comparison with catalysts based on carbon nanotubes). Additionally, for this catalyst after high-temperature modification with silver, the highest signal intensity ratio IG/ID = 7.83 is observed, which indirectly indicates an insufficient interaction of silver with the carbon nanotube substrate. The MWCNT_Ag 10% catalyst is characterized by a high degree of change in the structure of carbon nanotubes based on the signal intensity ratio IG/ID = 2.45, which can lead to a closer contact of the electron density of silver with the electronic configuration of the carbon substrate and, consequently, to increased efficiency in the reaction of electroreduction of oxygen from an alkaline electrolyte.

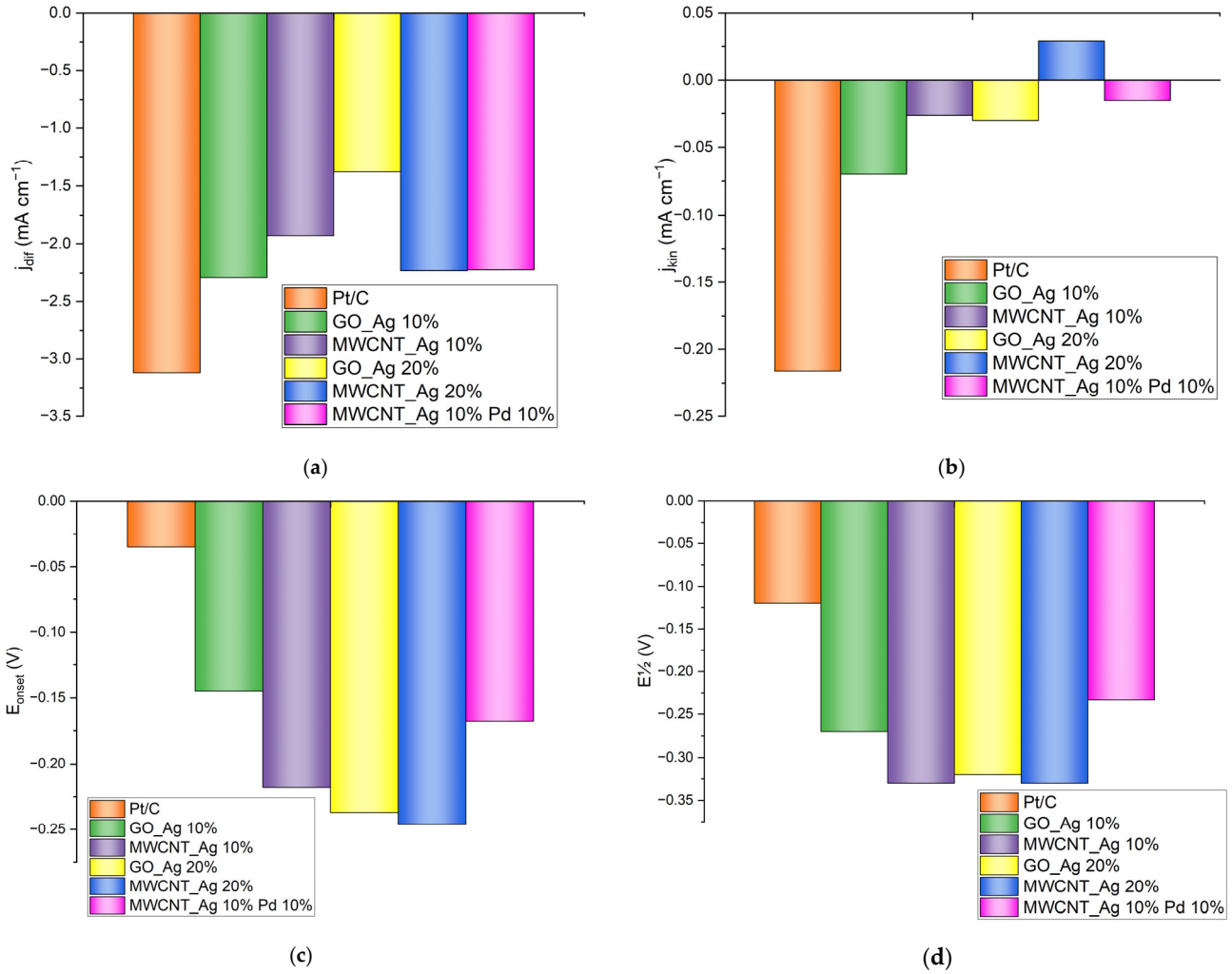

Figure 7. Comparative diagrams for synthesized catalysts and commercial platinum catalyst: (**a**) current densities in the diffusion region, (**b**) current densities in the kinetic region, (**c**) initial potential, (**d**) half-wave potential.

The addition of palladium increased the half-wave potential to $E_{1/2} = -0.23$ and the initial potential to $E_{onset} = -0.218$, which exceeds the characteristics of the monometallic catalysts except GO_Ag 10%, which has a higher initial potential. This is probably due to the fact that this MWCNT_Ag 10% Pd 10% catalyst is characterized by a rather high specific surface area (20.8 m^2/g) and a rather low IG/ID ratio = 3.46. It was noticed that at the subsequent modification with palladium of a silver catalyst on the base of CNTs, the cathodic peak on the linear voltammetry diagram at the potential of 0.080 V disappears. This peak is present in silver electrocatalysts and is associated with the reduction of silver oxide (Ag_2O) [20]. Apparently, in the MWCNT_Ag 10% Pd 10% catalyst there are not separate metal phases of palladium and silver, but there is a phase of bimetallic alloy of a certain composition.

The values of current density in the kinetic region for the obtained catalysts differ greatly from the values of this attribute for the commercial platinum catalyst (Pt/C), which indicates their lower catalytic activity. The GO-based catalyst containing 10% wt.% silver exhibits high activity and shows high current density values among all synthesized catalysts.

In the diffusion region, the values of current densities of the synthesized catalysts are quite close to those of the commercial platinum catalyst. The GO_Ag 10%, MWCNT_Ag 20% and MWCNT_Ag 10% Pd 10% catalysts are the closest to the platinum catalyst.

Based on the diagrams of linear voltammetry at different speeds of rotation of the disk electrode (500–2000 rpm), dependencies are plotted in the coordinates of the Koutecky–Levich equation. With an increase in the speed of rotation of the disk electrode, the current density increases, which indirectly indicates the diffusion kinetics of the reaction of electroreduction of oxygen from an alkaline electrolyte.

The number of electrons was calculated using the Koutecky–Levich equation:

$$\frac{1}{j} = \frac{1}{j_k} + \frac{1}{j_d} = \frac{-1}{nFkc_{O_2}} - \frac{1}{0.62nFD_{O_2}^{2/3}\vartheta^{-1/6}c_{O_2}\omega^{1/2}}$$

j—measured current density;
j_k, j_d—kinetic and limited diffusion current densities;
k—electrochemical rate constant of oxygen reduction;
D_{O_2}—oxygen diffusion coefficient (1.9×10^{-5} $cm^2 \cdot s^{-1}$);
c_{O_2}—the concentration of oxygen in the volume;
ϑ—kinematic viscosity of the solution;
ω—angular velocity of rotation of the electrode;
n—the number of electrons transferred per oxygen molecule.

Figure 8 shows the dependences in the Koutecky–Levich coordinates for the synthesized catalysts plotted using the parameters of the oxygen reduction reaction at different rotation speeds of the disk electrode in an oxygen-saturated 0.1 M KOH solution.

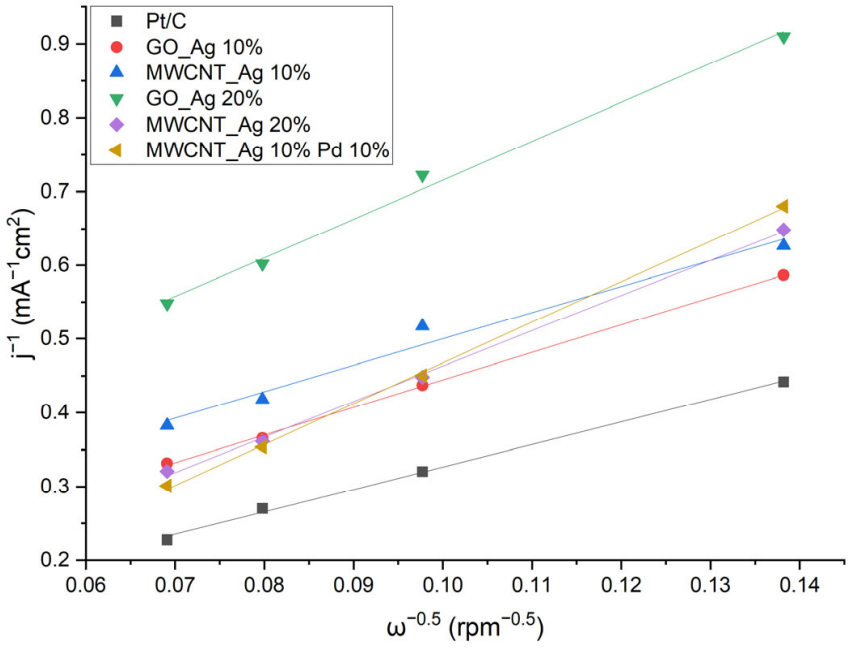

Figure 8. Dependences in coordinates of the Koutecky–Levich equation potential −0.8 V for the synthesized catalysts.

The linear form of the obtained dependences indirectly indicates the diffusion-limiting stage of the oxygen electroreduction process. Extrapolation of the dependencies leads to non-zero values of the reverse current, which may confirm the mixed kinetics of the process of electroreduction of oxygen from an alkali on the synthesized catalysts. Based on these dependences, we calculated the number of electrons (n) involved in the electrochemical reaction under study, shown in Figure 9.

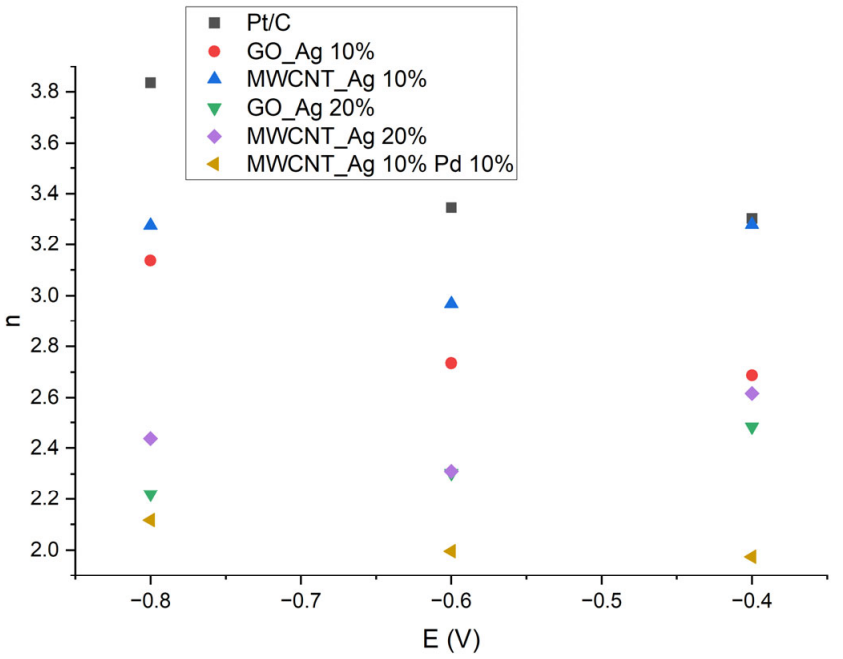

Figure 9. Dependence of the number of electrons transferred in the oxygen reduction reaction on the potential.

The MWCNT_Ag 10% and GO_Ag 10% catalysts showed the best results. For these samples, the electroreduction of oxygen at a potential of −0.8 V is characterized by the number of transferred electrons of about 3.3 and 3.1, respectively. This fact indicates the preferential formation of water as the main reaction product and the low yield of HO_2^-.

The two most active catalysts were tested for stability by cyclic voltammogram in the range of $-1.0 \div 0.2$ V with a sweep of 100 mV/s.

After 1000 cycles in an electrolyte saturated with oxygen, the current density in the diffusion region decreased by a small amount of ~7% for GO_Ag 10% and ~3% for MWCNT_Ag 10% Pd 10%. Thus, the addition of palladium leads to an increase in the stability of the catalyst. This may be due to the fact that probably in the bimetallic catalyst MWCNT_Ag 10% Pd 10% there is a palladium–silver alloy of a certain composition resistant to corrosion. The LV samples are shown in Figure 10.

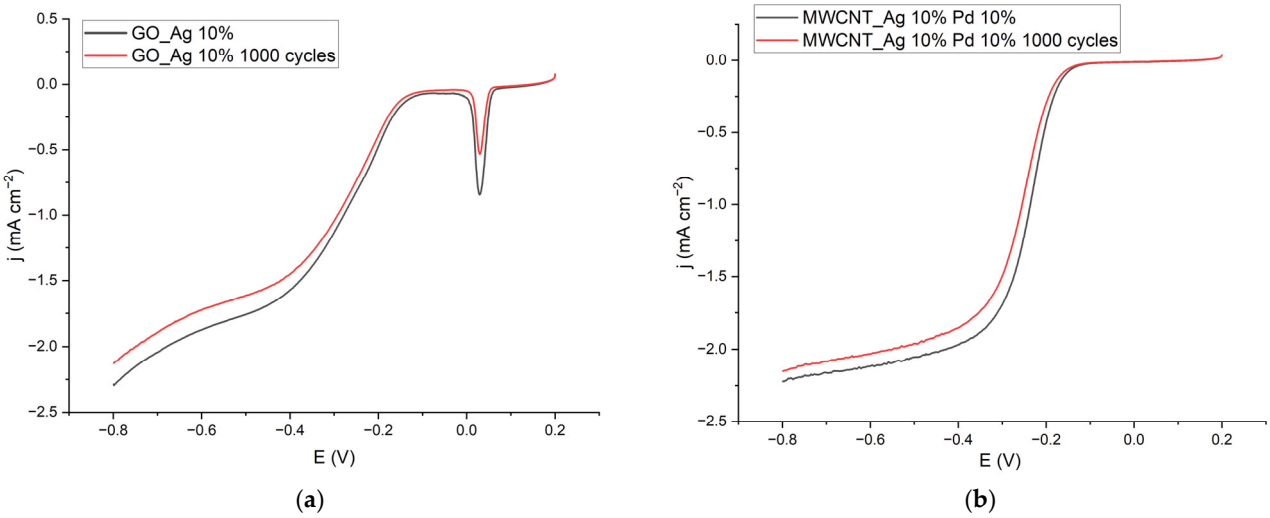

Figure 10. Corrosion testing of the most active catalysts: (**a**) GO Ag 10%, (**b**) MWCNT_Ag 10% Pd 10%.

Detailed results of corrosion tests are shown in Table 4. It can be seen that for the samples there is a slight decrease in the initial potential; however, the effect on the half-wave potential is ambiguous. For GO_Ag 10%, the potential increases, and for MWCNT_Ag 10% Pd 10%, there is a decrease.

Table 4. Characteristics of catalysts before and after corrosion testing.

Catalyst	E1/2, V (vs. Ag/AgCl)	j, mA cm^{-2} (E = −0.8 V)	E, V (j = 0.1 mA cm^{-2})
GO Ag 10%	−0.269	−2.287	−0.124
GO Ag 10% 1000 cycles	−0.266	−2.126	−0.140
MWCNT_Ag 10% Pd 10%	−0.233	−2.222	−0.157
MWCNT_Ag 10% Pd 10% 1000 cycles	−0.239	−2.152	−0.166

Table 5 presents the half-wave potentials for the catalysts studied in this work, as well as catalysts for which data are given in the literature.

Table 5. Half-wave potential for the catalysts given in this paper and in the literature.

Catalyst	E1/2,V (vs. Ag/AgCl)	E1/2,V (vs. SCE)	Source
GO_Ag 10%	−0.27	−0.32	
MWCNT_Ag 10%	−0.33	−0.38	
MWCNT_Ag 10% Pd 10%	−0.23	−0.28	
Ag/NGO1	−0.22	−0.26	[15]
Ag/NGO2	−0.22	−0.26	[15]
Ag/MWCNT1	−0.26	−0.31	[15]
Ag/MWCNT2	−0.27	−0.32	[15]
Pd@Ag/RGO	−0.17	−0.22	[21]

It can be seen that the properties of the obtained materials are similar to those of the materials presented in the literature.

4. Conclusions

Synthesized catalysts for the electroreduction of oxygen based on GO and MWCNTs modified with different amounts of silver and palladium were analyzed. It was shown that the modification of the carrier leads to a change in the textural characteristics of the catalyst. It was found that the silver particles on the carrier have different sizes, which can contribute to the formation of a wide range of the number of active centers. The highest activity was demonstrated by the catalyst based on graphene oxide modified with 10 wt.% silver showing the initial potency E_{onset} = −0.145 V. The MWCNT_Ag 10% Pd 10% catalyst showed the highest half-wave potential of E1/2 = −0.23 V; however, it was inferior to GO_Ag 10% using other indicators. In the diffusion region the GO_Ag 10%, MWCNT_Ag 20%, and MWCNT_Ad 10% Pd 10% catalysts show similar characteristics.

Author Contributions: Conceptualization, A.V.B. and R.V.S.; methodology, K.Y.V., V.V.P., A.A.S.-M., E.A.M., and E.O.T.; software, K.Y.V.; validation, A.V.B., R.V.S., and P.V.K.; formal analysis, A.V.B.; investigation, K.Y.V., N.A.V., and E.A.M.; resources, A.V.B.; data curation, R.V.S. and S.V.V.; writing—original draft preparation, K.Y.V.; writing—review and editing, A.V.B.; visualization, K.Y.V.; supervision, A.V.B.; project administration, A.V.B.; funding acquisition, A.V.B. All authors have read and agreed to the published version of the manuscript.

Funding: This study was carried out with the financial support of the Russian Foundation for Basic Research project no. 19–53-80033.

Data Availability Statement: Data obtained during this study are included in the main text.

Conflicts of Interest: The authors declare no conflict of interest.

References

1. Huya-Kouadio, J. *Doe Hydrogen and Fuel Cells Program Record*; US Departament of Energy: Washinton, DC, USA, 2017.
2. Truong, V.M.; Yang, M.K.; Yang, H. Functionalized carbon black supported silver (Ag/C) catalysts in cathode electrode for alkaline anion exchange membrane fuel cells. *Int. J. Precis. Eng. Manuf. Green Technol.* **2019**, *6*, 711–721. [CrossRef]
3. Kim, M.; Firestein, K.L.; Fernando, J.F.; Xu, X.; Lim, H.; Golberg, D.V.; Na, J.; Kim, J.; Nara, H.; Tang, J.; et al. Strategic design of Fe and N co-doped hierarchically porous carbon as superior ORR catalyst: From the perspective of nanoarchitectonics. *Chem. Sci.* **2022**, *13*, 10836–10845. [CrossRef] [PubMed]
4. Nasim, F.; Ali, H.; Nadeem, M.A.; Nadeem, M.A. High-performance FeO x@ CoO x/NC electrocatalysts for the oxygen reduction reaction in alkaline media. *Sustain. Energy Fuels* **2023**, *7*, 190–200. [CrossRef]
5. Sirirak, R.; Jarulertwathana, B.; Laokawee, V.; Susingrat, W.; Sarakonsri, T. FeNi alloy supported on nitrogen-doped graphene catalysts by polyol process for oxygen reduction reaction (ORR) in proton exchange membrane fuel cell (PEMFC) cathode. *Res. Chem. Intermed.* **2017**, *43*, 2905–2919. [CrossRef]
6. Jiang, L.; Hsu, A.; Chu, D.; Chen, R. A highly active Pd coated Ag electrocatalyst for oxygen reduction reactions in alkaline media. *Electrochim. Acta* **2010**, *55*, 4506–4511. [CrossRef]
7. Bharti, A.; Cheruvally, G. Influence of various carbon nano-forms as supports for Pt catalyst on proton exchange membrane fuel cell performance. *J. Power Sources* **2017**, *360*, 196–205. [CrossRef]
8. Ruiz-Camacho, B.; Palafox-Segoviano, J.A.; Pérez-Díaz, P.J.; Medina-Ramírez, A. Synthesis of supported Pt nanoparticles by sonication for ORR: Effect of the graphene oxide-carbon composite. *Int. J. Hydrogen Energy* **2021**, *46*, 26027–26039. [CrossRef]
9. Wang, T.; Chutia, A.; Brett, D.J.; Shearing, P.R.; He, G.; Chai, G.; Parkin, I.P. Palladium alloys used as electrocatalysts for the oxygen reduction reaction. *Energy Environ. Sci.* **2021**, *14*, 2639–2669. [CrossRef]
10. Sravani, B.; Raghavendra, P.; Chandrasekhar, Y.; Reddy, Y.V.M.; Sivasubramanian, R.; Venkateswarlu, K.; Madhavi, G.; Sarma, L.S. Immobilization of platinum-cobalt and platinum-nickel bimetallic nanoparticles on pomegranate peel extract-treated reduced graphene oxide as electrocatalysts for oxygen reduction reaction. *Int. J. Hydrogen Energy* **2020**, *45*, 7680–7690. [CrossRef]
11. He, X.; Li, D.; Bai, Z.; Chang, F.; Qiao, J.; Yang, L. Multi-wall carbon nanotube-supported palladium–cobalt oxide nanoparticle as efficient catalyst for oxygen reduction reaction. *Ionics* **2019**, *25*, 5929–5937. [CrossRef]
12. Ma, M.; Zhu, W.; Shao, Q.; Shi, H.; Liao, F.; Shao, C.; Shao, M. Palladium–copper bimetallic nanoparticles loaded on carbon black for oxygen reduction and zinc–air batteries. *ACS Appl. Nano Mater.* **2021**, *4*, 1478–1484. [CrossRef]
13. Zhao, K.; Shu, Y.; Li, F.; Peng, G. Bimetallic catalysts as electrocatalytic cathode materials for the oxygen reduction reaction in microbial fuel cell: A review. *Green Energy Environ.* **2022**. [CrossRef]
14. Ruiz-Camacho, B.; Medina-Ramírez, A.; Fuentes-Ramírez, R.; Navarro, R.; Goméz, C.M.; Pérez-Larios, A. Pt and Pt–Ag nanoparticles supported on carbon nanotubes (CNT) for oxygen reduction reaction in alkaline medium. *Int. J. Hydrogen Energy* **2022**, *47*, 30147–30159. [CrossRef]
15. Linge, J.; Erikson, H.; Merisalu, M.; Sammelselg, V.; Tammeveski, K. Oxygen reduction on silver catalysts electrodeposited on various nanocarbon supports. *SN Appl. Sci.* **2021**, *3*, 263. [CrossRef]
16. Qi, L.; Tang, X.; Wang, Z.; Peng, X. Pore characterization of different types of coal from coal and gas outburst disaster sites using low temperature nitrogen adsorption approach. *Int. J. Min. Sci. Technol.* **2017**, *27*, 371–377. [CrossRef]
17. Li, F.; Cao, B.; Zhu, W.; Song, H.; Wang, K.; Li, C. Hydrogenation of phenol over Pt/CNTs: The effects of Pt loading and reaction solvents. *Catalysts* **2017**, *7*, 145. [CrossRef]
18. Damdinov, B.B.; Ershov, A.A.; Krylov, A.S.; Maksimova, O.M.; Vtyurin, A.N. Investigation of silver nanoparticles by Raman scattering. In Proceedings of the XXXIV Session of the Russian Acoustic Society, Moscow, Russia, 14–18 February 2022; pp. 1192–1197. [CrossRef]
19. Wu, J.; Zhang, D.; Wang, Y.; Hou, B. Electrocatalytic activity of nitrogen-doped graphene synthesized via a one-pot hydrothermal process towards oxygen reduction reaction. *J. Power Sources* **2013**, *227*, 185–190. [CrossRef]
20. Shafigulin, R.V.; Tokranova, E.O.; Bulanova, A.V.; Kazakevich, P.V.; Vostrikov, S.V.; Martynenko, E.A.; Zhu, H. Carbon black modified with silver and low concentration of palladium as effective catalysts for electroreduction of oxygen in alkaline solutions. *React. Kinet. Mech. Catal.* **2021**, *133*, 455–465. [CrossRef]
21. Raghavendra, P.; Reddy, G.V.; Sivasubramanian, R.; Chandana, P.S.; Sarma, L.S. Reduced graphene oxide-supported Pd@ Au bimetallic nano electrocatalyst for enhanced oxygen reduction reaction in alkaline media. *Int. J. Hydrogen Energy* **2018**, *43*, 4125–4135. [CrossRef]